Activation of Inflammasomes Requires Intracellular Redistribution of the Apoptotic Speck-Like Protein Containing a Caspase Recruitment Domain[1]

Nicole B. Bryan,*† Andrea Dorfleutner,* Yon Rojanasakul,‡ and Christian Stehlik[2]*

Activation of caspase 1 is essential for the maturation and release of IL-1β and IL-18 and occurs in multiprotein complexes, referred to as inflammasomes. The apoptosis-associated speck-like protein containing a caspase recruitment domain (ASC) is the essential adaptor protein for recruiting pro-caspase 1 into inflammasomes, and consistently gene ablation of ASC abolishes caspase 1 activation and secretion of IL-1β and IL-18. However, distribution of endogenous ASC has not yet been examined in detail. In the present study, we demonstrated that ASC localized primarily to the nucleus in resting human monocytes/macrophages. Upon pathogen infection, ASC rapidly redistributed to the cytosol, followed by assembly of perinuclear aggregates, containing several inflammasome components, including caspase 1 and Nod-like receptors. Prevention of ASC cytosolic redistribution completely abolished pathogen-induced inflammasome activity, which affirmed that cytosolic localization of ASC is essential for inflammasome function. Thus, our study characterized a novel mechanism of inflammasome regulation in host defense. ***The Journal of Immunology,*** **2009, 182: 3173–3182.**

Inflammatory reactions in response to pathogen infection are highly coordinated processes. Leukocytes are recruited to sites of infection where they become activated and enlist tissue cells to aid with pathogen clearance. This response is orchestrated by a complex array of soluble mediators, including locally released cytokines and chemokines, such as macrophage-released IL-1β and IL-18. Generation of mature IL-1β and IL-18 is regulated at multiple steps, including transcription, posttranslational processing, and receptor binding (1). Processing into the bioactive secreted 17- or 18-kDa forms is dependent on the proteolytic activity of caspase 1, which itself becomes activated in molecular platforms, referred to as inflammasomes (2). Inflammasomes emerged recently as multiprotein complexes that link recognition of damage-associated molecular patterns (DAMPs)[3] by members of the Nod-like receptor (NLR) family of cytosolic pattern recognition receptors to the activation of caspase 1 and processing and release of the proinflammatory cytokines IL-1β and IL-18 (3–8). Core inflammasome proteins therefore include NLRs, the pyrin domain (PYD) and caspase recruitment domain (CARD)-containing adaptor protein apoptotic speck-like protein containing a CARD (ASC), and caspase 1 (2, 9). The inflammasome-initiating event is recognition of intracellular DAMPs derived from pathogens (pathogen-associated molecular pattern (PAMPs) or host (danger or stress signals) by a cytosolic NLR. Thus, inflammasomes are assumed to form in the cytosol of phagocytic cells such as monocytes and macrophages. NLRs undergo ATP-dependent oligomerization in response to DAMP recognition and recruit ASC by PYD-PYD interaction (10, 11). Subsequently, caspase 1 is recruited through the CARD of ASC, which is essential for its activation (12, 13). Consistently, macrophages deficient in ASC are impaired in their ability to activate caspase 1 in response to infection and tissue damage, emphasizing its central role for the activation of inflammatory caspases (14, 15).

NLRP3 (cryopyrin) is activated by Gram-positive bacteria and multiple DAMPs including MDP, bacterial and viral RNA, toxins that cause a decrease in intracellular potassium levels, genomic DNA, irritants, such as trinitrochlorobenzene and dinitro-1-fluorobenzene and reactive oxygen species, as well as uric acid and calcium pyrophosphate crystals (16–22). NLRP3 also functions in concert with P2X7 receptors recognizing extracellular ATP (17, 20). Due to the central role of IL-1β and IL-18 in regulating inflammation and immunity, dysregulation of pathways leading to caspase 1 activation and the resulting uncontrolled secretion of these proinflammatory mediators is directly linked to human inflammatory disorders. Variants of NLRP1 are associated with autoimmune diseases that cluster with vitiligo (23). NLRP3-containing inflammasomes were recently linked to contact hypersensitivity, sunburn, essential hypertension, gout, and pseudogout, and elevated expression of NLRP3 is detected in synovial fluids of rheumatoid arthritis patients (19, 24–27). Furthermore, hereditary mutations in NLRP3 rendering the protein constitutively active, are directly linked to cryopyrin-associated periodic syndromes (28, 29). Mutant NLRP3 proteins efficiently form complexes with ASC to mediate caspase 1 activation independent of an

*Division of Rheumatology, Department of Medicine, Feinberg School of Medicine, Northwestern University, Chicago, IL 60611; †Program in Cancer Cell Biology, Health Sciences Center, West Virginia University, Morgantown, WV 26506; ‡Department of Pharmaceutical Sciences, School of Pharmacy, Health Sciences Center, West Virginia University, Morgantown, WV 26506

Received for publication July 18, 2008. Accepted for publication January 4, 2009.

The costs of publication of this article were defrayed in part by the payment of page charges. This article must therefore be hereby marked *advertisement* in accordance with 18 U.S.C. Section 1734 solely to indicate this fact.

[1] This project was supported by National Institutes of Health Grants 1R21AI067680, 1R03AI067806, and 1R21AI082406 from the National Institute of Allergy and Infectious Diseases, Grant 1R01GM071723 from the National Institute of General Medical Sciences, the American Heart Association (Grant 0950125G), The Concern Foundation, and the John P. Gallagher Research Professorship.

[2] Address correspondence and reprint requests to Dr. Christian Stehlik, Division of Rheumatology, Department of Medicine, Feinberg School of Medicine, Northwestern University, 240 East Huron, McGaw Pavilion, Chicago, IL 60611. E-mail address: c-stehlik@northwestern.edu

[3] Abbreviations used in this paper: DAMP, damage-associated molecular pattern; NLR, Nod-like receptor; PYD, pyrin domain; CARD, caspase recruitment domain; PAMP, pathogen-associated molecular pattern; ASC, apoptotic speck-like protein containing a CARD; NLS, nuclear localization sequence; siRNA, small interfering RNA; HKLP, heat-killed *Legionella pneumophila*; HKSA, heat-killed *Staphylococcus aureus*; DAPI, 4′,6-diamidino-2-phenylindole; shRNA, short hairpin RNA.

www.jimmunol.org/cgi/doi/10.4049/jimmunol.0802367

activating ligand. This finding demonstrates the potential benefits of controlling the accessibility of ASC for cytosolic NLRs (30). Several mechanisms have been proposed by which activation of inflammasomes might be regulated, including single PYD or CARD-containing proteins and pyrin (30). However, regulation of inflammasomes still remains largely elusive.

In this study, we describe a novel regulatory mechanism for inflammasome assembly. We propose that ASC is sequestered in the nucleus in resting monocytes and macrophages and only becomes available to bridge NLRs and caspase 1 in the cytosol, once macrophages are activated in response to pathogen infection and cellular stress. Such a mechanism might provide an additional safety checkpoint to limit spontaneous activation of caspase 1 in resting cells.

Materials and Methods

Cell culture

THP-1, U-937, HL-60, and HEK293 cells were obtained from the American Type Culture Collection and maintained as recommended by American Type Culture Collection. HEK293 cells were transiently transfected using Polyfect (Qiagen) according to the manufacturer's instructions. THP-1 cells were used at low passage numbers and were regularly tested for *Mycoplasma* infection (MycoAlert; Lonza). THP-1 cells were transiently transfected using the Nucleofector II (Amaxa) with solution V and protocol V001 using two ASC-specific small interfering RNAs (siRNAs) targeting the 3′ untranslated region and nt 474–492 of the ASC open reading frame (31). THP-1 cells were seeded into collagen I (5 μg/cm^2)-coated glass coverslips and differentiated into adherent macrophages by overnight culture in medium supplemented with 15 ng/ml PMA and further cultured for 2 days. Where indicated, cells were treated with 2 μg/ml *Escherichia coli* total RNA (Ambion) or 2×10^5 CFU/ml heat-killed *Legionella pneumophila* (HKLP) or *Staphylococcus aureus* (HKSA; InvivoGen).

Isolation of primary monocytes from human peripheral blood

Human monocytes were isolated by Ficoll-Hypaque centrifugation (Sigma-Aldrich) from heparinized blood. Mononuclear cells were removed, washed, and resuspended in serum-free DMEM and isolated by adherence to plastic dishes. Adherent monocytes were washed, incubated in complete RPMI 1640 medium overnight in glass chamber slides, and left untreated or treated with 2 μg/ml *E. coli* total RNA (Ambion). Macrophages were obtained by culture of adherent monocytes on collagen type I (5 μg/cm^2)-coated glass coverslips for 7 days in medium containing 20% FBS. Alternatively, monocytes were isolated from PBMCs by countercurrent centrifugal elutriation in the presence of 10 μg/ml polymyxin B sulfate using a JE-6B rotor (Beckman Coulter).

Expression plasmids

The nuclear localization sequence (NLS) from the SV40 large T Ag (DPKKKRKV) was used to generate a 3xNLS-ASC fusion protein with red fluorescent protein (RFP) epitope tags in pcDNA3 (Invitrogen) and pMSCV-puro (Clontech) expression vectors (32). Three silent point mutations were introduced in the siRNA recognition sequence (QuickChange; Stratagene) to prevent siRNA-mediated degradation of ASC and NLS-ASC. Authenticity of all plasmids was confirmed by sequencing. All other plasmids have been previously described (33).

Retroviral infections

293GP2 cells (Clontech) were transiently transfected with RFP-tagged ASC, NLS-ASC, empty pMSCV-puro, or GFP-ASC in modified pMSCV-puro expression vectors (Clontech) or pRNATin-H1.4 (Genscript) in combination with a vesicular stomatitis virus (VSV) G-encoding expression plasmid to produce a pseudo-typed recombinant retrovirus. THP-1 cells (5×10^5) were infected by spinoculation in the presence of 6 μg/ml polybrene (Sigma-Aldrich) at 32°C. Stable cells were selected 72 h after infection with 3 μg/ml puromycin or 400 μg/ml hygromycin for 14 days. Expression of ASC and NLS-ASC was verified in pooled cell populations by immunoblot, and knockdown of ASC was verified by immunoblot in cells sorted by FACS for coral GFP expression.

Generation of short hairpin RNA (shRNA) plasmids

shRNA expression constructs were generated by inserting double-stranded oligonucleotides into the *Mlu*I and *Xho*I sites of pRNATin-H1.4 (Genscript) downstream of the RNA polymerase III H1 promoter. Stable knockdown of ASC in THP-1 cells was achieved by infection with a VSV-G-pseudo-typed retrovirus encoding a shRNA targeting ASC (targeting sequence gctcttcagtttcacacca) or firefly luciferase (targeting sequence gatttcgagtcgtcttaat) as control by spinoculation on 3 consecutive days. Cells were selected in hygromycin (400 μg/ml) for 14 days and sorted by FACS for coral GFP expression, which is encoded in the vector backbone independent from the shRNA.

Immunofluorescence microscopy

Adherent cells on collagen I-coated coverslips (5 μg/cm^2) were fixed in 3.7% paraformaldehyde, incubated in 50 mM glycine for 5 min, and permeabilized and blocked with 0.5% saponin, 1.5% BSA, and 1.5% normal goat serum for 30 min. ASC was immunostained with affinity-purified monoclonal anti-ASC Abs (1 μg/ml; MBL) directed to the PYD, affinity-purified polyclonal Abs directed to the CARD from Chemicon, Calbiochem, and Apotech (1/200), custom-made affinity-purified polyclonal Abs directed to the linker (CS3; 1/2500), and monoclonal anti-myc Abs (1/350; Santa Cruz Biotechnology). Caspase 1 was immunostained with a monoclonal anti-caspase 1 Ab from BD Biosciences (1/500) and a polyclonal Ab from Santa Cruz Biotechnology (1/50); NLRP3 was immunostained with monoclonal anti-NLRP3 Abs from Abcam (1/50) and Santa Cruz Biotechnology (1/50); and IL-1β with a polyclonal Ab from Santa Cruz Biotechnology (1/50). Secondary Alexa Fluor 488, 546, and 647-conjugated Abs, ToPro-3, 4′,6-diamidino-2-phenylindole (DAPI), and phalloidin were from Molecular Probes. Cells were washed with PBS containing 0.5% saponin, and coverslips were mounted using Fluoromount-G (Southern Biotechnology Associates). Suspension cells were fixed and stained as above and adhered to poly-L-lysine-coated slides using a cytocentrifuge (StatSpin). Images were acquired by confocal laser-scanning microscopy on a Zeiss LSM 510 or LSM 510 Meta and epifluorescence microscopy on a Nikon TE2000E2 with a ×100 oil immersion objective and image deconvolution.

Subcellular fractionation

Cells (10^6) were resuspended in hypotonic lysis buffer (10 mM Tris-HCl (pH 7.4), 10 mM NaCl, 3 mM $MgCl_2$, 1 mM EDTA, and 1 mM EGTA supplemented with protease and phosphatase inhibitors), incubated on ice, adjusted to 250 mM sucrose, and lysed in a Dounce homogenizer. Samples were initially centrifuged at 4ºC at $1000 \times g$ for 3 min to remove any intact cells and then centrifuged at 4ºC at $2000 \times g$ for 10 min to pellet the nuclei. The cytosolic supernatant was removed, and the nuclear pellet was then washed three times in hypotonic lysis buffer with the addition of 250 mM sucrose and 0.1% Nonidet P-40 and incubated for 20 min on ice. Both fractions were adjusted to 50 mM Tris-HCl (pH 7.4), 20 mM NaCl, 3 mM $MgCl_2$, 250 mM sucrose, 0.5% deoxycholate, 0.1% SDS, 0.2% Nonidet P-40, and protease and phosphatase inhibitors and fully solubilized by brief sonication. Fifty micrograms of protein lysates was separated by SDS-PAGE, transferred to a polyvinylidene difluoride membrane, and probed with anti-ASC Abs (CS3) and HRP-conjugated secondary Abs (Amersham Pharmacia) in conjunction with an ECL detection system (Pierce). Membranes were stripped and reprobed with anti-GAPDH (Sigma-Aldrich) and anti-Lamin A (Santa Cruz Biotechnology) Abs as control for cytosolic and nuclear fractions, respectively.

Measurement of secreted IL-1β

IL-1β secretion was quantified in culture supernatants using a commercial ELISA (BD Biosciences) at least in triplicates. Briefly, primary macrophages or THP-1 cells were treated with *E. coli* total RNA (2 μg/ml), 2×10^5 CFU/ml HKLP or 2×10^5 CFU/ml heat-killed *Staphylococcus aureus* (HKSA; InvivoGen) in 12-well dishes for 16 h and the cleared culture supernatant was analyzed by ELISA. HEK293 cells were grown in collagen I-treated 12-well culture dishes and cotransfected with plasmids encoding mouse pro-IL-1β, pro-caspase-1, NLRP3^{R260W}, ASC, or NLS-ASC. Twenty-four hours posttransfection, culture medium was replaced, collected 36 h posttransfection, and clarified, and IL-1β activated by reconstituted inflammasomes was analyzed by mouse IL-1β ELISA according to the manufacturer's protocol (13, 33, 34).

Statistical methods

A standard two-tailed t test was used for statistical analysis; values of $p \leq 0.05$ were considered significant.

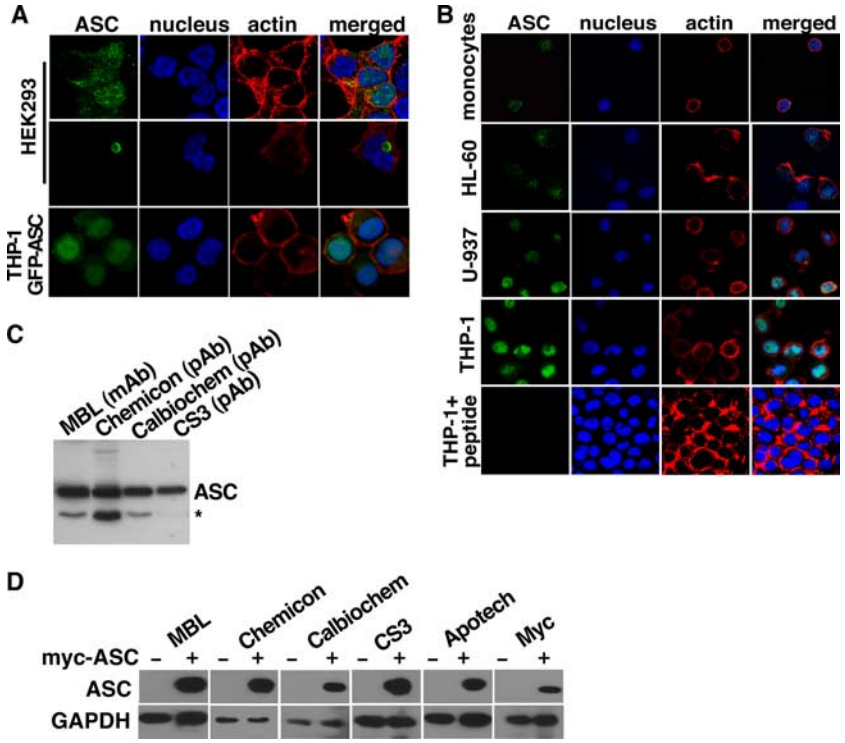

FIGURE 1. Nuclear localization of ASC. *A*, HEK293 cells were transiently transfected with myc-ASC, fixed, and immunostained with anti-myc and Alexa Fluor 488-conjugated Abs, while GFP-ASC-expressing THP-1 cells were fixed and cytospun onto glass slides. ASC either localized diffusely throughout the cell (*upper panel*) or into a perinuclear aggregate (*middle panel*), while stable expression of GFP-ASC in THP-1 cells showed nuclear localization (*lower panel*). *B*, Subcellular localization of endogenous ASC was examined in primary human monocytes and several monocytic cell lines. Cells were fixed and ASC was immunostained with mAbs from MBL (monocytes; *first panel*) and polyclonal Abs from Chemicon, Calbiochem, and custom-made (HL-60, U-937, THP-1; *second*, *third*, and *fourth panels*, respectively). THP-1 cells were also immunostained in the presence of a 1000x molar excess of the ASC-specific peptide that is recognized by the CS3 anti-ASC Ab (*fifth panel*). Secondary Alexa Fluor 488-conjugated Abs were used in combination with ToPro-3 and Alexa Fluor 546-conjugated phalloidin to counterstain nuclei (DNA) and the actin cytoskeleton to outline cells, respectively. Images were acquired by laser-scanning confocal microscopy, and the *panels* from *left* to *right* are showing ASC (green), nucleus (blue), actin (red), and a merged image. *C*, THP-1 lysates (75 μg) were analyzed by immunoblot with the anti-ASC Abs used in immunofluorescence microscopy. An asterisk denotes a splice form of ASC, which is not recognized by our custom-made polyclonal anti-ASC Ab (CS3). *D*, HEK293T cells were either mock transfected or transfected with a myc-tagged ASC expression construct. Cleared cell lysates were analyzed by immunoblot using the anti-ASC Abs used in immunofluorescence microscopy and anti-myc Abs (Santa Cruz Biotechnology) as control. Blots were also stripped and reprobed for GAPDH to demonstrate equal loading.

Results

Nuclear localization of ASC in resting monocytes

ASC has previously been shown to localize diffusely throughout the cell (Fig. 1*A*, *upper panel*) and to form characteristic aggregates (Fig. 1*A*, *middle panel*) (35). In addition, THP-1 cells stably expressing GFP-ASC predominantly exhibited nuclear distribution of GFP-ASC, as determined by nuclear counter staining (Fig. 1*A*, *lower panel*). However, most studies to date have relied upon overexpression of ASC. To clarify the localization of ASC and its implications on the activity of inflammasomes, we studied the subcellular localization of endogenous ASC in monocytes and macrophages, where it is essential for inflammasome function (14, 15). First, we examined ASC subcellular localization by immunofluorescence microscopy in primary human peripheral blood monocytes (Fig. 1*B*, *first panel*) and a panel of human monocytic cell lines, including HL-60 (Fig. 1*B*, *second panel*), U-937 (Fig. 1*B*, *third panel*), and THP-1 (Fig. 1*B*, *fourth panel*). Without exception, all cells showed nuclear localization of ASC, emphasizing that endogenous ASC localized to the nucleus in monocytes. Immunostaining was performed with different anti-ASC Abs, including commercially available mouse monoclonal (U-937) or rabbit polyclonal (HL-60) Abs or a custom-made rabbit polyclonal anti-ASC Ab (THP-1 and primary monocytes). To further demonstrate specificity of nuclear ASC staining, we performed an ASC peptide competition assay. The custom-made polyclonal anti-ASC Ab was incubated with a 1000-fold molar excess of the peptide used initially for immunization before being used in immunostaining of THP-1 cells (Fig. 1*B*, *fifth panel*). Peptide competition completely abrogated nuclear ASC staining in THP-1 cells. These ASC Abs are highly specific for ASC without cross-reactivity by Western blot of THP-1 cell lysates (Fig. 1*C*) and HEK293 cells that were transfected with myc-tagged ASC or control plasmid (Fig. 1*D*).

Stimulation-dependent translocation of ASC from the nucleus to the cytosol in monocytes

Inflammasomes form in response to pathogen and PAMP recognition, and we therefore examined the localization of ASC in primary monocytes and THP-1 monocytes after treatment with *E. coli* total RNA for 30 min, which specifically activates a NLRP3-dependent inflammasome response (20, 36). Contrary to the nuclear localization of ASC observed in resting monocytes (Fig. 1*B*), immunofluorescence staining of *E. coli* total RNA-activated cells revealed a cytosolic distribution of ASC in primary as well as THP-1 monocytes (Fig. 2*A*). To confirm this observation, proteins from resting and *E. coli* total RNA-treated THP-1 cells were fractionated into nuclear and cytosolic fractions and immunoblotted with

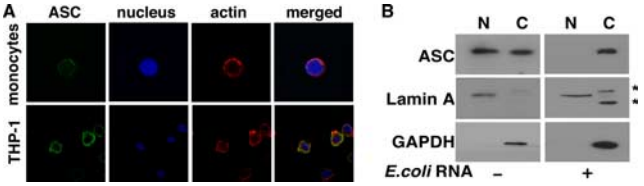

FIGURE 2. Cytosolic redistribution of ASC in response to inflammatory stimulation of monocytes. *A*, Subcellular localization of ASC was analyzed by immunofluorescence in primary monocytes and THP-1 monocytes following treatment with *E. coli* total RNA (2 μg/ml) for 30 min using the monoclonal anti-ASC Ab described in Fig. 1. Images were acquired by laser-scanning confocal microscopy. *Panels* from *left* to *right* are showing ASC (green), nucleus (blue), actin (red), and a merged image. *B*, Subcellular localization of ASC was determined by subcellular fractionation of control and *E. coli* total RNA (2 μg/ml)-activated THP-1 cells. 10^6 cells were fractionated by differential centrifugation into nuclear (N) and cytosolic (C) fractions, and protein lysates (50 μg) were analyzed by immunoblotting with anti-ASC and HRP-conjugated secondary Abs. Fractionation efficiency was controlled by reprobing membranes with anti-GAPDH (cytosolic) and anti-Lamin A (nuclear) Abs. *, Two cross-reactive proteins in the cytosolic fraction following *E. coli* total RNA treatment.

ASC-specific Abs. To control fractionation efficiency, membranes were stripped and reprobed with Abs specific for the cytosolic GAPDH and the nuclear Lamin A proteins, respectively (Fig. 2*B*). Although the control proteins clearly indicated that the fractionation procedure was highly efficient, ASC was also seen in the cytosol in resting cells, which was not visible by immunofluorescence microscopy and was likely caused by nuclear leakage of the small ASC protein during aqueous fractionation, which is a well-acknowledged problem for small proteins (37, 38). ASC is only 22 kDa in size and therefore retaining >50% of ASC inside the nucleus during fractionation further confirms its predominantly nuclear localization in resting monocytes, and that ASC redistributes from the nucleus to the cytosol following exposure to *E. coli* total RNA. Therefore, we conclude that PAMPs are capable of inducing translocation of ASC from the nucleus to the cytosol in monocytes.

Formation of cytosolic ASC aggregates in response to inflammatory activation of macrophages

Monocytes infiltrate sites of infection and differentiate into inflammatory macrophages to aid pathogen clearance and homeostasis. Therefore, we next examined distribution of ASC in primary macrophages, which were either resting or activated with *E. coli* total RNA for 6 h. Similar to monocytes, resting macrophages displayed primarily nuclear ASC (Fig. 3*A*, *upper panel*), while the majority of *E. coli* total RNA-activated macrophages showed the characteristic ASC-containing perinuclear aggregates (Fig. 3*A*, *lower panel*), reminiscent of the structures that were observed upon ASC overexpression (Fig. 1*A*, *middle panel*). To prove that THP-1 cells can be used as a model for inflammasome studies, ASC-containing aggregates were also assessed in PMA-differentiated THP-1 macrophages by immunostaining before and after activation with *E. coli* total RNA for 6 h. As observed for primary macrophages, differentiated resting THP-1 macrophages showed nuclear ASC (Fig. 3*B*, *upper panel*) and activation with *E. coli* total RNA for 6 h caused ASC to form cytosolic aggregates (Fig. 3*B*, *middle panel*). To demonstrate specificity for the staining of ASC-containing aggregates, we also performed a peptide competition assay with the custom-made rabbit polyclonal anti-ASC Ab, as shown in Fig. 1*B*. Peptide competition completely abrogated any ASC aggregate staining (Fig. 3*B*, *lower panel*), which confirmed the specificity of the ASC Ab for ASC aggregate staining. Since ASC is the only known adaptor protein for inflammasome-mediated caspase 1 activation, ASC-containing aggregate formation may be crucial for caspase 1 activation and, consequently, macrophages from $ASC^{-/-}$ mice fail to activate caspase 1 in response to Gram-positive and Gram-negative bacteria (14). Gram-positive but not Gram-negative pathogens are able to induce inflammasomes in an ASC- and NLRP3-dependent manner (14, 17, 20, 39). To demonstrate that the observed response is not only due to a PAMP, THP-1-derived macrophages were infected with heat-killed Gram-positive *S. aureus* (HKSA) for 4 h, followed by immunofluorescence staining of ASC. Concomitant with NLRP3-dependent pathogen recognition and subsequent inflammasome formation and activation, Gram-positive pathogens also caused ASC aggregate formation (Fig. 3*C*, *upper panel*). Additionally, Gram-negative HKLP,

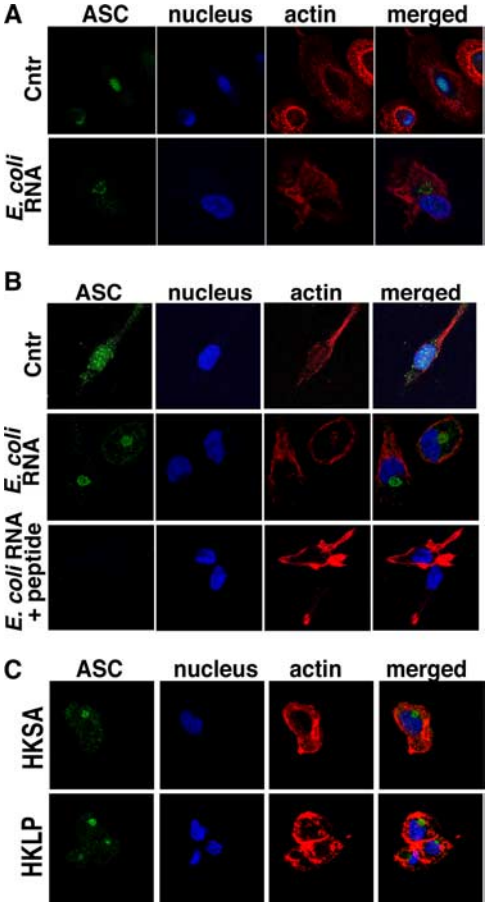

FIGURE 3. Aggregate formation of endogenous ASC in response to inflammatory stimulation in macrophages. Subcellular localization of ASC was analyzed by immunofluorescence in primary macrophages (*A*) and PMA-differentiated THP-1 macrophages (*B* and *C*) using mono- and polyclonal anti-ASC and Alexa Fluor 488-conjugated secondary Abs in combination with ToPro-3 nuclear stain and Alexa Fluor 546-conjugated phalloidin to visualize actin. Images were acquired by laser-scanning confocal microscopy. All *panels* show ASC (green), nucleus (blue), actin (red), and a merged image from *left* to *right*. *A*, Primary macrophages, either untreated (*upper panel*) or *E. coli* total RNA treated (2 μg/ml; *lower panel*), were immunostained using the CS3 polyclonal anti-ASC Ab. *B*, Untreated (*upper panel*) and *E. coli* total RNA (2 μg/ml)-treated THP-1 macrophages (*middle* and *lower panels*) were immunostained using the polyclonal anti-ASC Ab in the absence (*middle panel*) or in the presence (*lower panel*) of a 1000× molar excess of the ASC-specific peptide (note the loss of specific ASC aggregate staining in the panel with peptide competition). *C*, THP-1 macrophages were activated with 2×10^5 CFU/ml HKSA (*upper panel*) and HKLP (*lower panel*) and immunostained with the CS3 polyclonal Ab. Cntr, Control.

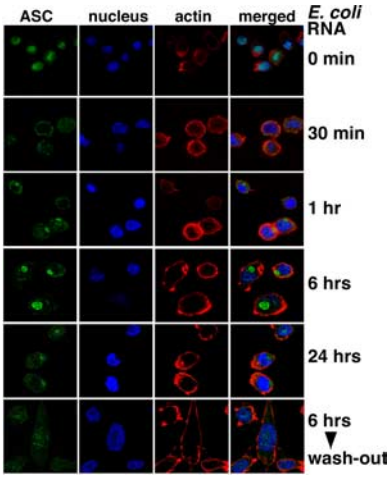

FIGURE 4. Aggregation of ASC occurs within 1 h of inflammatory stimulation of macrophages and depends on the continued presence of the stimulus. Subcellular localization of ASC in THP-1 macrophages was analyzed by immunofluorescence following stimulation of cells with *E. coli* total RNA (2 μg/ml) for the indicated times. Cells were fixed at 0 min, 30 min, 1 h, 6 h, and 24 h poststimulation. In addition, after 6 h of stimulation, cells were washed extensively and cultured for an additional 12 h in the absence of *E. coli* total RNA. Fixed cells were stained with the polyclonal CS3 anti-ASC and Alexa Fluor 488-conjugated secondary Abs. DNA and the actin cytoskeleton were visualized as above. The *panels* from *left* to *right* are showing ASC (green), nucleus (blue), actin (red), and a merged image.

for which no specific NLR has been defined yet, also caused ASC-containing aggregates (Fig. 3*C*, *lower panel*). These data suggest that inflammasomes potentially activated by other NLRs are able to trigger ASC aggregate formation, which is therefore not limited to NLRP3.

ASC aggregation is an early response of macrophage activation

Maturation and release of IL-1β by macrophages occurs rapidly in response to infections. We therefore wanted to investigate a time course of ASC nuclear to cytosolic redistribution and formation of aggregates in response to stimulation with *E. coli* RNA. THP-1 cells were kept untreated or treated with *E. coli* total RNA for 0.5, 1, 6, and 24 h, and distribution of ASC was analyzed in these cells by immunofluorescence (Fig. 4). Within 30 min of *E. coli* total RNA treatment, the majority of cells displayed ASC redistribution from the nucleus to the cytosol, with some cells showing diffuse nuclear and cytosolic distribution. After 1 h, ASC was cytosolic, with aggregate formation visible in some cells. Longer exposure to *E. coli* total RNA induced ASC-containing aggregates in the majority of cells and further increased the size of these aggregates, which are still present after 24+ hours of activation, without any signs of toxicity. Significantly, duration of ASC-containing aggregates required the persistent presence of *E. coli* total RNA (or LPS or heat-killed pathogens; data not shown), since washout of *E. coli* RNA after 6 h of exposure caused a dissociation of aggregates with some nuclear accumulation of ASC visible after 12 h (Fig. 4, *lower panel*). This observation suggested that ASC redistribution and aggregation is reversible, which could indicate a function in host response to infections and other stress situations.

Caspase 1 and NLRP3 colocalize with ASC to aggregates

Inflammasomes are multiprotein complexes consisting of at least a NLR protein, ASC, and caspase 1 (2). Overexpression studies suggested that many ASC-interacting proteins colocalize to aggregates of overexpressed ASC. We find that, in response to pathogen infection, macrophages display a 4- to 6-μm ring-shaped perinuclear structure which contains endogenous ASC (Fig. 5*A*). Upon compiling 20 images along the *z*-axis, a three-dimensional image revealed that this structure is spherical with a hollow center (Fig. 5*B*). To characterize localization of additional inflammasome proteins, immunostaining for caspase 1 and NLRP3 was performed. In resting THP-1 macrophages, caspase 1 localized to the nucleus and to small vesicular structures in the cytosol (Fig. 5*C*, *upper panel*), while *E. coli* total RNA activation caused partial localization of caspase 1 to perinuclear aggregates (Fig. 5*C*, *lower panel*). Costaining of caspase 1 with ASC showed that both proteins displayed a similar pattern inside the nucleus in resting THP-1 macrophages (Fig. 5*D*, *upper panel*) and that both proteins colocalize to aggregates in *E. coli* total RNA-treated cells (Fig. 5*D*, *lower panel*). NLRP3^{R260W} is a constitutively active cryopyrin-associated periodic syndrome-linked mutant causing ligand-independent recruitment of ASC and caspase 1 (40, 41). Coexpression of ASC, pro-caspase 1, and NLRP3^{R260W} in HEK293 cells caused formation of ASC-containing aggregates and colocalization of all three inflammasome proteins in these aggregates (Fig. 5*E*). We did not obtain specific staining for endogenous NLRP3 in resting cells, which is in agreement with reports that NLRP3 is inducibly expressed in response to proinflammatory agents (42). Nevertheless, in *E. coli* total RNA-treated cells, NLRP3 was present in ASC-containing aggregates in some cells, as well as in punctate structures throughout the cytosol (Fig. 5*F*). Overall, these results demonstrate that macrophages recruit NLRs, ASC, and caspase 1 into perinuclear aggregates in response to pathogen infection, providing the intriguing possibility that these aggregates may represent inflammasomes.

ASC aggregate-dependent maturation of IL-1β

To test the hypothesis that these aggregates may represent inflammasomes, we determined IL-1β secretion in cell culture supernatants by ELISA under conditions that cause ASC-containing aggregate formation in *E. coli* total RNA-treated macrophages (Fig. 6*A*). Secreted IL-1β was significantly elevated in macrophages after *E. coli* total RNA treatment over untreated control. To directly link elevated levels of released IL-1β to inflammasomes, we generated stable THP-1 cells with a shRNA-mediated knockdown of ASC. shRNA ASC or control THP-1 cells were treated with *E. coli* total RNA, HKLP or HKSA that cause ASC aggregate formation and secreted IL-1β levels were determined by ELISA in culture supernatants. Although control cells show a significant increase in secreted IL-1β, ASC knockdown cells are completely impaired in the release of IL-1β into culture supernatants (Fig. 6*B*). The efficiency of ASC knockdown was assessed by immunoblot in cleared lysates of control and ASC knockdown cells (Fig. 6*B*). Furthermore, wild-type cells (GFP negative) form ASC-containing aggregates, as determined by immunofluorescence analysis, whereas ASC knockdown THP-1 cells (GFP-positive) do not show ASC-containing aggregates following *E. coli* total RNA treatment, further demonstrating the link between ASC-containing aggregates and IL-1β release (Fig. 6*C*).

Redistribution of ASC to the cytosol is essential for inflammasome activity

The significance of cytosolic redistribution of ASC is further emphasized by the cytosolic distribution of the inflammasome target pro-IL-1β in response to *E. coli* total RNA treatment of THP-1 cells. Consistent with previous reports that show up-regulated pro-IL-1β expression in response to infection (43), no IL-1β staining

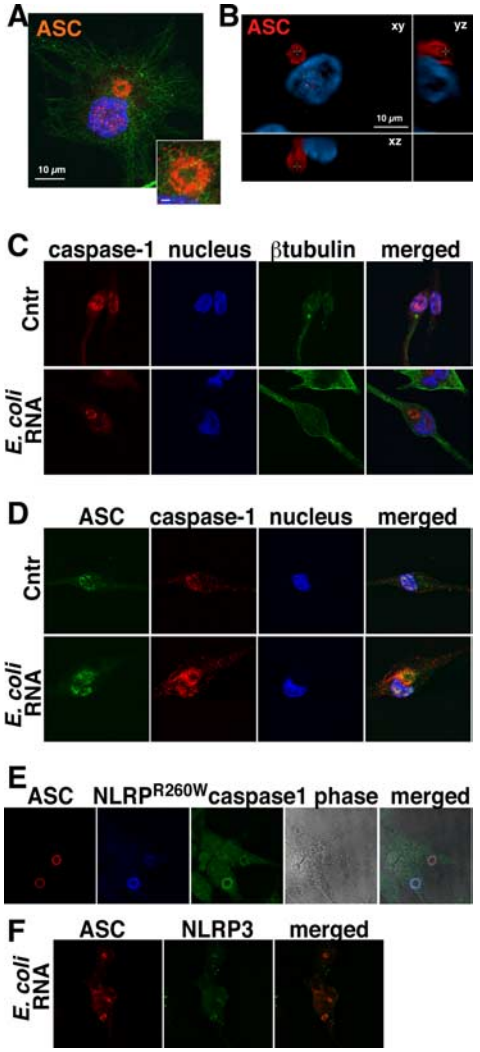

FIGURE 5. Caspase 1 and NLRP3 colocalize with ASC in aggregates. All images show PMA-differentiated THP-1 macrophages, except *E*, which are HEK293T cells. *A*, Cells were treated with *E. coli* total RNA (2 μg/ml) and immunostained with polyclonal anti-ASC and Alexa Fluor 546-conjugated Abs (red), monoclonal anti-β-tubulin and Alexa Fluor 488-conjugated Abs (green), and the nuclear stain DAPI (blue). The *inset* in the *lower right half* highlights the ring-shaped ASC-containing aggregate. The scale bar measures 10 and 1 μm, respectively. *B*, *E. coli* total RNA (2 μg/ml)-treated cells were immunostained with polyclonal anti-ASC and Alexa Fluor 546-conjugated Abs (red) and DAPI (blue). Twenty optical sections at 0.6 μm were captured, deconvoluted, and assembled into a three-dimensional structure showing xy, yz, and xz views of the aggregate. The scale bar is 10 μm. *C* and *D*, Untreated (*upper panel*) or *E. coli* total RNA (2 μg/ml)-treated cells (*lower panel*) were fixed and immunostained with polyclonal anti-caspase 1 and monoclonal β-tubulin and Alexa Fluor 546- and 488-conjugated secondary Abs (*C*), respectively. *D*, Polyclonal anti-ASC and monoclonal anti-caspase 1 Abs and Alexa Fluor 488- and 546-conjugated secondary Abs, respectively. DNA was visualized with DAPI and *panels* from *left* to *right* show (*C*) caspase 1 (red), nucleus (blue), β-tubulin (green), and a merged image and (*D*) ASC (green), caspase 1 (red), nucleus (blue), and a merged image. *E*, Flag-tagged ASC, hemagglutinin-tagged caspase 1, and myc-tagged NLRP3^{R260W} were transiently transfected into HEK293 cells and immunostained with rabbit anti-ASC, mouse anti-NLRP3, and rat anti-HA Abs, and Alexa Fluor 546-, 647-, and 488-conjugated secondary Abs, respectively, to determine colocalization of all three proteins in transfected cells. *Panels* from *left* to *right* show ASC (red), NLRP3^{R260W} (blue), caspase 1 (green), phase, and a merged image. *F*, *E. coli* total RNA (2 μg/ml)-treated THP-1 macrophages were immunostained with rabbit anti-ASC and goat anti-NLRP3 Abs and Alexa Fluor 488- and 546-conjugated secondary Abs, respectively. *Panels* from *left* to *right* show ASC (red) and NLRP3 (green) and a merged image.

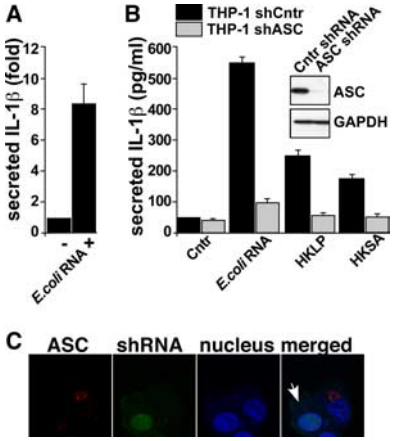

FIGURE 6. ASC aggregate formation is linked to the maturation of IL-1β. *A*, Normalized culture supernatants from resting and *E. coli* RNA (2 μg/ml)-activated primary human macrophages were analyzed by ELISA for released IL-1β. Results represent an average of two independent experiments and are presented as fold release compared with untreated macrophages. *B*, Culture supernatants from THP-1 cells stably transfected with either a shRNA targeting ASC (■) or a control shRNA targeting luciferase (▨) and left either untreated or treated with *E. coli* RNA (2 μg/ml), HKLP (2×10^5 CFU/ml), or HKSA (2×10^5 CFU/ml) were analyzed as above for released IL-1β. Cells were previously FACS sorted for GFP expression, which is encoded from the pRNATin-H1.4 (Genscript) shRNA vector backbone. Results represent an average of three independent experiments and are presented as pg/ml of released IL-1β. The *inset* shows an immunoblot of control shRNA- and ASC shRNA-expressing THP-1 cells for ASC and GAPDH as a loading control. *C*, ASC-containing aggregates were analyzed following treatment with *E. coli* total RNA (2 μg/ml) for 6 h by immunofluorescence in a mixed population of shRNA ASC-transfected cells before FACS sorting for GFP expression of the ASC shRNA. ASC was immunostained with the polyclonal CS3 Ab, and images were acquired by laser-scanning confocal microscopy. *Panel* shows from *left* to *right* ASC (red), ASC shRNA (green), nucleus (blue), and a merged image. Note that the cell on the left side (white arrow) encodes the ASC shRNA, as indicated by the GFP positive signal and therefore does not form ASC-containing aggregates, while the cell on the right is GFP negative, thus does not encode the ASC shRNA and therefore shows aggregated ASC.

was observed in resting cells (Fig. 7*A*, *upper panel*), while cytosolic distribution is present in activated cells (Fig. 7*A*, *lower panel*). To further test the hypothesis that ASC cytosolic redistribution is essential for inflammasome formation and activity, we altered its intracellular localization. A constitutive nuclear ASC was generated by in-frame fusion of ASC with three tandem repeats of the strong consensus NLS derived from the SV40 large T Ag, which has frequently been used to target proteins to the nucleus (32, 44). Three copies of the NLS were used to ensure efficient nuclear retention of ASC even after inflammatory stimulation. We chose this approach over mutational analysis because both death domain folds of ASC require correct folding to retain full adaptor function and even point mutations could disrupt the overall structure and function of ASC, which may lead to a wrong interpretation of results, while NH_2-terminal fusion of ASC generally does not alter its function (data not shown). To confirm the nuclear localization of this ASC fusion protein (NLS-ASC), HEK293 cells were transfected and localization was compared with wild-type ASC. As shown in Fig. 1*A*, overexpression of wild-type ASC results in either nuclear/cytosolic localization or preferentially the formation of perinuclear aggregates (Figs. 1*A* and 7*B*, *upper panels*). In contrast, transfection of NLS-ASC showed exclusively nuclear localization, suggesting that the fusion of a strong NLS to ASC was sufficient to retain it inside the nucleus

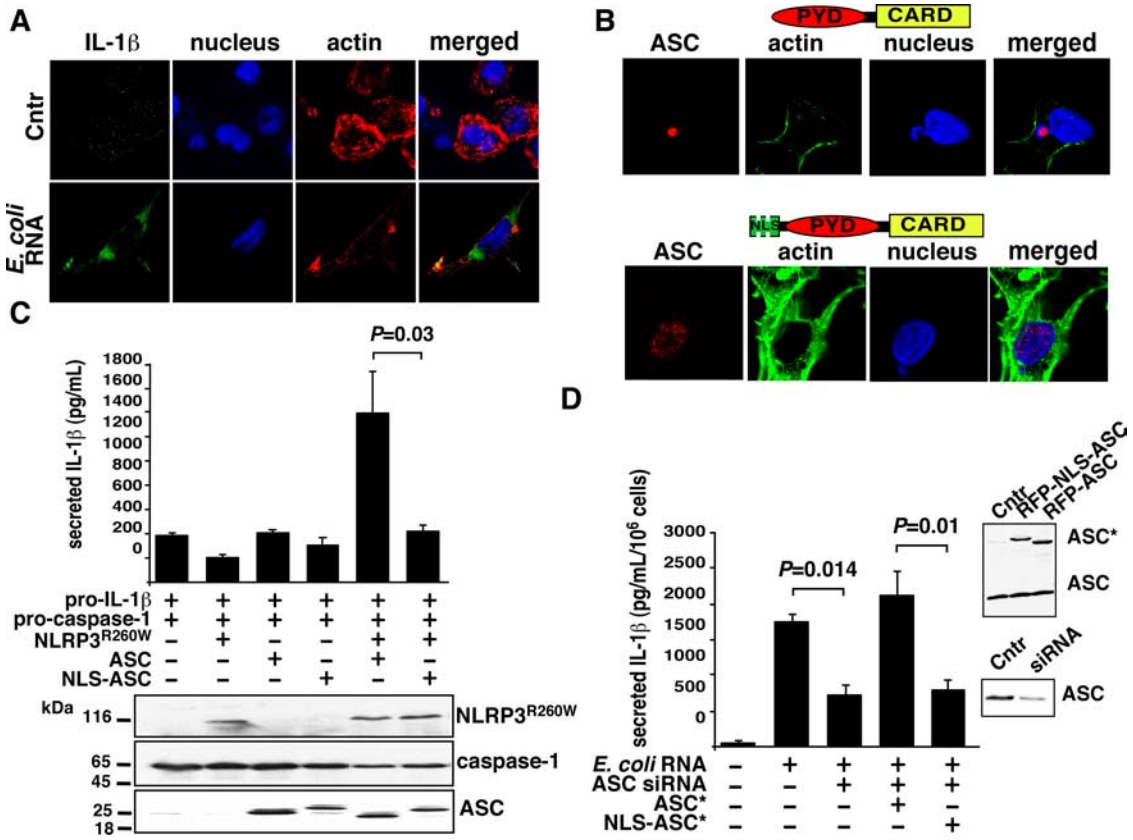

FIGURE 7. ASC localization to the cytosol is required for inflammasome formation and efficient IL-1β secretion. *A*, Untreated and *E. coli* RNA-treated THP-1 macrophages were immunostained with anti-IL-1β and Alexa Fluor 488-conjugated secondary Abs. Nuclei and actin were visualized as above. *Panels* show from *left* to *right* IL-1β (green), nucleus (blue), actin (red), and a merged image. *B*, Myc-tagged ASC (*upper panel*) and myc-tagged NLS-ASC (*lower panel*) were transiently transfected into HEK293 cells and immunostained with monoclonal anti-myc and Alexa Fluor 546-conjugated secondary Abs. Nuclei and actin were visualized as above. *Panels* show from *left* to *right* ASC (red), actin (green), nucleus (blue), and a merged image. Images in *A* and *B* were acquired by laser-scanning confocal microscopy. *C*, Inflammasomes consisting of a constitutively active NLRP3^{R260W}, pro-IL-1β, pro-caspase 1, and either ASC or NLS-ASC were transiently reconstituted in HEK293 cells, as indicated, and inflammasome activity was assayed by analyzing secreted IL-1β by ELISA. Results represent an average of at least three independent experiments $\pm$ SD. Cleared and normalized cellular lysates were analyzed by immunoblot for expression of all transfected inflammasome components as indicated. *D*, THP-1 cells were stably infected with a VSV-G pseudo-typed recombinant retrovirus encoding either RFP-fused ASC or RFP-fused NLS-ASC with expression levels comparable to endogenous ASC. Mock-infected, RFP-ASC, and RFP-NLS-ASC-expressing cells were transiently transfected with two pooled ASC-specific siRNAs to knockdown expression of endogenous ASC, but not RFP-ASC or RFP-NLS-ASC. Cells were seeded into fresh wells 24 h after nucleofection and where indicated treated with LPS and *E. coli* RNA for 12 h. Secreted IL-1β was determined in culture supernatants by ELISA and results are presented as pg/ml of 10^6 cells and represent an average of three independent experiments $\pm$ SD. The *inset* shows stable expression of RFP-ASC and RFP-NLS-ASC compared with endogenous ASC in THP-1 cells (*upper panel*) and the siRNA-mediated reduction of endogenous ASC (*lower panel*) by immunoblot. An asterisk denotes expression of ASC and NLS-ASC containing silent point mutations in the sequence recognized by the siRNA preventing its degradation. Cntr, Control.

(Fig. 7*B*, *lower panel*). To determine the functional significance of nuclear vs cytosolic distribution of ASC, we used an inflammasome reconstitution assay in HEK293 cells, which are deficient in endogenous inflammasomes, but are able to produce mature IL-1β upon reconstitution of inflammasomes (13, 33, 34). We reconstituted inflammasomes by transient transfection of pro-caspase-1, pro-IL-1β, NLRP3^{R260W}, and either ASC or NLS-ASC and determined the amount of secreted IL-1β in culture supernatants. Although inflammasomes containing wild-type ASC caused processing and release of IL-1β, inflammasomes restored with NLS-ASC were not capable of secreting IL-1β into culture supernatants above baseline level (Fig. 7*C*). Total cell lysates were used to verify expression of all transfected inflammasome proteins by immunoblotting (Fig. 7*C*). To directly assess inflammasome activity in macrophages, we infected THP-1 cells with recombinant retroviruses encoding ASC or NLS-ASC, which is not targeted by the siRNA, because we introduced three silent point mutations in the siRNA recognition sequence. We used an RFP fusion to conveniently distinguish between endogenous and ectopic ASC by the increased molecular mass and chose stable, pooled cell populations with expression levels comparable to endogenous ASC, as analyzed by immunoblotting (Fig. 7*D*, *right upper panel*). Endogenous ASC was knocked down by two pooled siRNAs and was confirmed by immunoblotting (Fig. 7*D*, *right lower panel*). Next, IL-1β release was measured in response to *E. coli* total RNA treatment. Although activation of control cells strongly promoted release of IL-1β, knockdown of endogenous ASC from wild-type cells efficiently reduced IL-1β release, which was restored in RFP-ASC-expressing cells. In contrast, expression of NLS-ASC in ASC knockdown cells failed to restore secretion of IL-1β above the level observed in stimulated ASC knockdown cells (Fig. 7*D*, *left panel*). These data confirmed that nuclear export of ASC is essential for inflammasome activity, since nuclear retention of ASC completely impaired inflammasome-mediated IL-1β release.

Discussion

In this report, we studied the intracellular distribution of the central inflammasome adaptor ASC and provide evidence that inducible

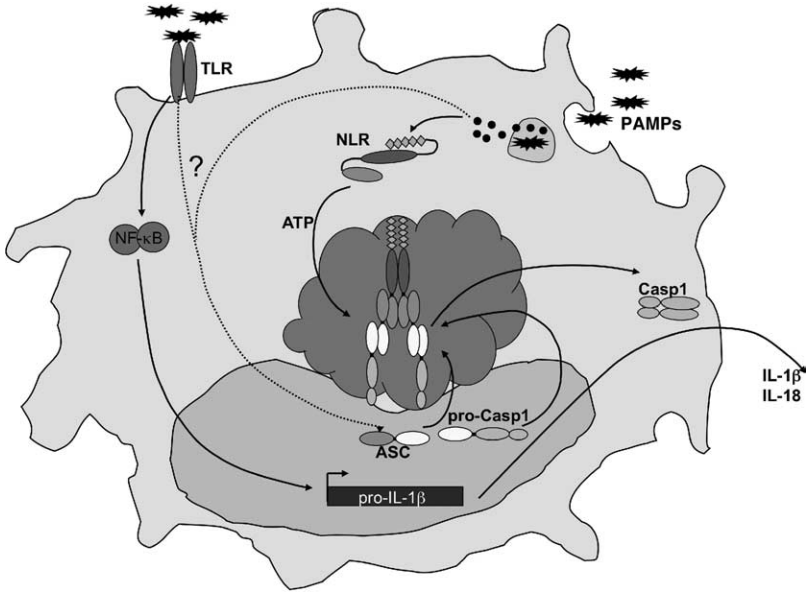

FIGURE 8. A model for inflammasome formation and activation. Cross-talk between the TLR and NLR system has been proposed, where initial DAMP recognition by TLRs triggers transcriptional up-regulation of pro-IL-1β and other inflammasome components. Subsequently, DAMP recognition by NLRs is required for maturation of pro-IL-1β and pro-IL-18. Our data indicate that DAMP recognition also causes redistribution of ASC from the nucleus to the cytosol by a yet elusive mechanism, which then can be recruited to activated NLRs to assemble inflammasomes. The perinuclear aggregates in activated macrophages contain the core inflammasome proteins and might represent inflammasomes.

redistribution of ASC from the nucleus to the cytosol is essential for inflammasome function. Although inflammasomes are biochemically characterized, no detailed studies have been undertaken to visualize endogenous inflammasomes. Overexpression studies result predominantly in the formation of aggregates, referred to as specks (35, 45). However, ASC-containing aggregates were believed to represent artificial results driven by enforced overexpression causing self-aggregation of ASC. We observed nuclear localization of ASC in monocytes and macrophages with several anti-ASC Abs recognizing different epitopes, thus excluding epitope masking as an explanation for our results.

Nuclear localization of ASC, however, cannot explain its essential function as an adaptor protein for inflammasome-mediated caspase 1 activation, which occurs in the cytosol of cells (46). We find cytosolic accumulation of ASC in response to purified PAMPs as well as heat-killed Gram-negative and Gram-positive bacteria, suggesting that this response is part of the host defense to clear pathogens. Redistribution of ASC from the nucleus to the cytosol can be observed as early as 30 min poststimulation, while longer stimulation caused the aggregation of ASC into structures that resembled the specks observed by enforced overexpression of ASC, including the perinuclear localization and the spherical morphology with a hollow center. Additionally, ASC-containing aggregates appear to grow in size over time. To our knowledge, we provide the first evidence of host defense-mediated assembly of endogenous ASC-containing aggregates in macrophages. We propose that inducible redistribution of ASC from the nucleus to the cytosol is required for its interaction with activated NLRs to form caspase 1-activating inflammasomes. ASC-containing aggregates not only assembled in response to the NLRP3 ligands bacterial RNA, and *S. aureus*, but also in response to Gram-negative bacteria and other PAMPs (data not shown), suggesting that other NLRs also aggregate with ASC, consistent with the requirement of ASC for inflammasome-mediated activation of caspase 1 in response to Gram-negative and Gram-positive pathogens (14).

Caspase 1 activation can induce pyroptosis, which is a form of programmed cell death associated with antimicrobial responses in inflammation, which results in osmotic lysis of cells (47). A caspase 1 and GFP-ASC-containing protein complex termed pyroptosome has recently been proposed to facilitate pyroptosis through self-oligomerization of ASC in response to potassium depletion (45). However, other reports did not find a link between ASC and pyroptosis (48). NLRP3 and ASC have also been implicated in caspase 1- and IL-1β-independent pyronecrosis (49). Thus, the role of ASC- and caspase 1-containing complexes in pyroptosis and pyronecrosis is still unclear. We propose that ASC may participate in different multiprotein complexes that facilitate either effective IL-1β secretion (inflammasomes) or cell death (pyroptosomes, pyronecrosomes). ASC has also been shown to localize to mitochondria in response to genotoxic insult, which is essential to facilitate p53-mediated Bax translocation to mitochondria and subsequently apoptosis in fibroblasts, hence participating in yet another signaling complex (50). This complex could be specific to DNA damage in fibroblasts.

Although we do not understand yet what the determining factor for such different outcomes is in macrophages, we noticed significant differences in the appearance and functional properties of these multiprotein complexes. Endogenous ASC aggregates in response to NLR activation are 4–6 μm compared with the smaller ($\sim$1 μm) and more compact aggregates (specks) caused by overexpression of ASC and potassium depletion (45), or that form in response to cytotoxic treatment of macrophages (data not shown). Despite aggregate formation, cells do not show any sign of cell death for at least 48 h, which is in sharp contrast to the rapid cell death in response to the formation of GFP-ASC-containing pyroptosomes (45). ASC-containing aggregates are reversible, which is contrary to structures causing cell death, because removal of the activating ligand by washing in culture medium resulted in dissociation of ASC-containing aggregates and diffuse cytoplasmic and even nuclear redistribution of ASC. Furthermore, these complexes contain caspase 1 and NLRs, although caspase 1 colocalization with ASC was more frequently detectable than colocalization with NLRP3. Ultrastructural studies performed by electron microscopy and molecular approaches investigating the release of IL-1β from activated monocytes also did not find any signs of cell death during IL-1β release and suggested a secretory mechanism that does not involve apoptosis, cell death, or surface membrane lysis (51, 52).

Since conditions that induced ASC aggregates also caused maturation of IL-1β and IL-18, these ASC-containing aggregates could potentially represent inflammasomes. Inflammasomes have been biochemically characterized as large, inducible protein aggregates, consisting of a NLR, ASC, and pro-caspase 1 (2). Other

proteins can be associated with some inflammasomes. Thus, ASC-containing aggregates might provide a scaffold for inflammasome proteins to interact and to promote caspase 1 activation. Activation of NLRs causes their unfolding and NTP-mediated oligomerization, resulting in pentameric and heptameric aggregates in vitro (11). Thus, it is feasible that ASC aggregates might denote higher order oligomeric structures of NLRs, as indicated by their larger size. Alternatively, larger aggregates might assemble in vivo, because incorporation of accessory proteins is lacking by in vitro reconstitution. Recombinant NLRP1 pentamers or heptamers are ~20 nm in diameter (11), while most endogenous ASC aggregates are 4–6 μm. Adherence of cells is not required for ASC-containing aggregates, as we observed it also in activated monocytes (data not shown).

Fusion of proteins with nuclear localization sequences has been widely used to prevent redistribution of proteins with nuclear and cytosolic localization. We used this approach to sequester ASC inside the nucleus of macrophages to prevent ASC export. Nuclear ASC completely abrogated endogenous as well as reconstituted inflammasome-mediated maturation of IL-1β, directly demonstrating the requirement for ASC redistribution for inflammasome activity. We also noted colocalization of ASC with procaspase 1 in the nucleus of resting macrophages, suggesting that both proteins might preassemble in the nucleus of cells even before oligomerization with activated NLRs in the cytosol. In addition, both also localized to ASC-containing aggregates in activated macrophages. Different localizations have been reported for caspases 1, including cytosolic, vesicular, nuclear, as well as the inner and outer face of plasma membranes, which likely reflect different activation states of cells (51, 53–55). Moreover, caspase 1 is responsible for its own secretion alongside its cytokine substrates (2, 56). Nuclear caspase 1 has been suggested to mediate apoptosis in tumor cells, but we did not observe apoptosis in macrophages, despite its nuclear localization (53). This is supported by our observation that resting macrophages showed nuclear caspase 1, while a cytosolic to nuclear translocation occurs in neuroblastomas undergoing apoptosis (55).

Whether ASC is only physically separated inside the nucleus to prevent its spontaneous recruitment to NLRs and subsequent secretion of inflammatory cytokines, or whether ASC performs inflammasome-independent functions inside the nucleus warrants further investigations. The related protein FADD, which links death receptors to caspase 8 activation in the cytosol, has been recently shown to localize to the nucleus in nonapoptotic cells and its export is required for caspases 8 activation (44, 57). Nuclear and cytosolic FADD is involved in genome surveillance and death receptor-mediated apoptosis, respectively. Nuclear FADD further regulates mitosis and proliferation of T cells (58). Likewise, cytosolic TRADD, another death domain fold-containing adaptor protein, participates in death receptor-mediated apoptosis, while nuclear localized TRADD mediates promyelocytic leukemia and p53-mediated apoptosis and interacts with STAT1-α to modulate IFN-γ signaling in macrophages (59, 60).

Recent evidence suggested a cross-talk between TLRs and the NLR system during host defense. Pathogen recognition by TLRs is required for up-regulation of inflammasome components and substrates, while subsequently the NLR system is essential for processing the cytokine precursors. Our data indicate another layer of complexity in the regulation of IL-1β and IL-18 maturation, where pathogen recognition initially triggers nuclear to cytosolic redistribution of the NLR adaptor ASC, which then links NLRs to caspase 1 activation in inflammasomes (Fig. 8). Although the molecular mechanism of ASC cytosolic redistribution is currently elusive, it potentially could be targeted for prevention of inflammasome-mediated inflammatory cytokine secretion in patients with periodic fever syndromes and other inflammatory conditions.

Acknowledgments

We thank Dr. Richard Pope for critical review of this manuscript and for providing human primary macrophages. Imaging was performed at West Virginia University and Northwestern University Imaging Core Facilities.

Disclosures

The authors have no financial conflict of interest.

References

1. Dinarello, C. A. 1998. Interleukin-1β, interleukin-18, and the interleukin-1β converting enzyme. *Ann. NY Acad. Sci.* 856: 1–11.
2. Martinon, F., K. Burns, and J. Tschopp. 2002. The inflammasome: a molecular platform triggering activation of inflammatory caspases and processing of proIL-1b. *Mol. Cell* 10: 417–426.
3. Stehlik, C. 2007. The PYRIN domain in signal transduction. *Curr. Protein Pept. Sci.* 8: 293–310.
4. Mariathasan, S., and D. M. Monack. 2007. Inflammasome adaptors and sensors: intracellular regulators of infection and inflammation. *Nat. Rev. Immunol.* 7: 31–40.
5. Ogura, Y., F. S. Sutterwala, and R. A. Flavell. 2006. The inflammasome: first line of the immune response to cell stress. *Cell* 126: 659–662.
6. Ting, J. P., D. L. Kastner, and H. M. Hoffman. 2006. CATERPILLERs, pyrin and hereditary immunological disorders. *Nat. Rev. Immunol.* 6: 183–195.
7. Franchi, L., C. McDonald, T. D. Kanneganti, A. Amer, and G. Nunez. 2006. Nucleotide-binding oligomerization domain-like receptors: intracellular pattern recognition molecules for pathogen detection and host defense. *J. Immunol.* 177: 3507–3513.
8. Martinon, F., O. Gaide, V. Petrilli, A. Mayor, and J. Tschopp. 2007. NALP Inflammasomes: a central role in innate immunity. *Semin. Immunopathol.* 29: 213–229.
9. Agostini, L., F. Martinon, K. Burns, M. F. McDermott, P. N. Hawkins, and J. Tschopp. 2004. NALP3 forms an IL-1β-processing inflammasome with increased activity in Muckle-Wells autoinflammatory disorder. *Immunity* 20: 319–325.
10. Duncan, J. A., D. T. Bergstralh, Y. Wang, S. B. Willingham, Z. Ye, A. G. Zimmermann, and J. P. Ting. 2007. Cryopyrin/NALP3 binds ATP/dATP, is an ATPase, and requires ATP binding to mediate inflammatory signaling. *Proc. Natl. Acad. Sci. USA* 104: 8041–8046.
11. Faustin, B., L. Lartigue, J. M. Bruey, F. Luciano, E. Sergienko, B. Bailly-Maitre, N. Volkmann, D. Hanein, I. Rouiller, and J. C. Reed. 2007. Reconstituted NALP1 inflammasome reveals two-step mechanism of caspase-1 activation. *Mol. Cell* 25: 713–724.
12. Srinivasula, S. M., J.-L. Poyet, M. Razmara, P. Datta, Z. Zhang, and E. S. Alnemri. 2002. The PYRIN-CARD protein ASC is an activating adaptor for caspase-1. *J. Biol. Chem.* 277: 21119–21122.
13. Stehlik, C., S. H. Lee, A. Dorfleutner, A. Stassinopoulos, J. Sagara, and J. C. Reed. 2003. Apoptosis-associated speck-like protein containing a caspase recruitment domain is a regulator of procaspase-1 activation. *J. Immunol.* 171: 6154–6163.
14. Mariathasan, S., K. Newton, D. M. Monack, D. Vucic, D. M. French, W. P. Lee, M. Roose-Girma, S. Erickson, and V. M. Dixit. 2004. Differential activation of the inflammasome by caspase-1 adaptors ASC and Ipaf. *Nature* 430: 213–218.
15. Yamamoto, M., K. Yaginuma, H. Tsutsui, J. Sagara, X. Guan, E. Seki, K. Yasuda, M. Yamamoto, S. Akira, K. Nakanishi, et al. 2004. ASC is essential for LPS-induced activation of procaspase-1 independently of TLR-associated signal adaptor molecules. *Genes Cells* 9: 1055–1067.
16. Martinon, F., L. Agostini, E. Meylan, and J. Tschopp. 2004. Identification of bacterial muramyl dipeptide as activator of the NALP3/cryopyrin inflammasome. *Curr. Biol.* 14: 1929–1934.
17. Mariathasan, S., D. S. Weiss, K. Newton, J. McBride, K. O'Rourke, M. Roose-Girma, W. P. Lee, Y. Weinrauch, D. M. Monack, and V. M. Dixit. 2006. Cryopyrin activates the inflammasome in response to toxins and ATP. *Nature* 440: 228–232.
18. Sutterwala, F. S., Y. Ogura, M. Szczepanik, M. Lara-Tejero, G. S. Lichtenberger, E. P. Grant, J. Bertin, A. J. Coyle, J. E. Galan, P. W. Askenase, and R. A. Flavell. 2006. Critical role for NALP3/CIAS1/cryopyrin in innate and adaptive immunity through its regulation of caspase-1. *Immunity* 24: 317–327.
19. Watanabe, H., O. Gaide, V. Petrilli, F. Martinon, E. Contassot, S. Roques, J. A. Kummer, J. Tschopp, and L. E. French. 2007. Activation of the IL-1β-processing inflammasome is involved in contact hypersensitivity. *J. Invest. Dermatol.* 127: 1956–1963.
20. Kanneganti, T. D., N. Ozoren, M. Body-Malapel, A. Amer, J. H. Park, L. Franchi, J. Whitfield, W. Barchet, M. Colonna, P. Vandenabeele, et al. 2006. Bacterial RNA and small antiviral compounds activate caspase-1 through cryopyrin/Nalp3. *Nature* 440: 232–236.
21. Dostert, C., V. Petrilli, R. Van Bruggen, C. Steele, B. T. Mossman, and J. Tschopp. 2008. Innate immune activation through Nalp3 inflammasome sensing of asbestos and silica. *Science* 320: 674–677.

22. Muruve, D. A., V. Petrilli, A. K. Zaiss, L. R. White, S. A. Clark, P. J. Ross, R. J. Parks, and J. Tschopp. 2008. The inflammasome recognizes cytosolic microbial and host DNA and triggers an innate immune response. *Nature* 452: 103–107.
23. Jin, Y., C. M. Mailloux, K. Gowan, S. L. Riccardi, G. LaBerge, D. C. Bennett, P. R. Fain, and R. A. Spritz. 2007. NALP1 in vitiligo-associated multiple autoimmune disease. *N. Engl. J. Med.* 356: 1216–1225.
24. Martinon, F., V. Petrilli, A. Mayor, A. Tardivel, and J. Tschopp. 2006. Gout-associated uric acid crystals activate the NALP3 inflammasome. *Nature* 440: 237–241.
25. Omi, T., M. Kumada, T. Kamesaki, H. Okuda, L. Munkhtulga, Y. Yanagisawa, N. Utsumi, T. Gotoh, A. Hata, M. Soma, et al. 2006. An intronic variable number of tandem repeat polymorphisms of the cold-induced autoinflammatory syndrome 1 (CIAS1) gene modifies gene expression and is associated with essential hypertension. *Eur. J. Hum. Genet.* 14: 1295–1305.
26. Feldmeyer, L., M. Keller, G. Niklaus, D. Hohl, S. Werner, and H. D. Beer. 2007. The inflammasome mediates UVB-induced activation and secretion of interleukin-1β by keratinocytes. *Curr. Biol.* 17: 1140–1145.
27. Rosengren, S., H. M. Hoffman, W. Bugbee, and D. L. Boyle. 2005. Expression and regulation of cryopyrin and related proteins in rheumatoid arthritis synovium. *Ann. Rheum. Dis.* 64: 708–714.
28. Church, L. D., S. M. Churchman, P. N. Hawkins, and M. F. McDermott. 2006. Hereditary auto-inflammatory disorders and biologics. *Springer Semin. Immunopathol.* 27: 494–508.
29. Stojanov, S., and D. L. Kastner. 2005. Familial autoinflammatory diseases: genetics, pathogenesis and treatment. *Curr. Opin. Rheumatol.* 17: 586–599.
30. Stehlik, C., and A. Dorfleutner. 2007. COPs and POPs: Modulators of inflammasome activity. *J. Immunol.* 179: 7993–7998.
31. Stehlik, C., L. Fiorentino, A. Dorfleutner, J. M. Bruey, E. M. Ariza, J. Sagara, and J. C. Reed. 2002. The PAAD/PYRIN-family protein ASC is a dual regulator of a conserved step in nuclear factor κB activation pathways. *J. Exp. Med.* 196: 1605–1615.
32. Lanford, R. E., P. Kanda, and R. C. Kennedy. 1986. Induction of nuclear transport with a synthetic peptide homologous to the SV40 T antigen transport signal. *Cell* 46: 575–582.
33. Dorfleutner, A., N. B. Bryan, S. J. Talbott, K. N. Funya, S. L. Rellick, J. C. Reed, X. Shi, Y. Rojanasakul, D. C. Flynn, and C. Stehlik. 2007. Cellular PYRIN domain-only protein (cPOP) 2 is a candidate regulator of inflammasome activation. *Infect. Immun.* 75: 1484–1492.
34. Dorfleutner, A., S. J. McDonald, N. B. Bryan, K. N. Funya, J. C. Reed, X. Shi, D. C. Flynn, Y. Rojanasakul, and C. Stehlik. 2007. A Shope fibroma virus PYRIN-only protein modulates the host immune response. *Virus Genes* 35: 685–694.
35. Masumoto, J., S. Taniguchi, K. Ayukawa, H. Sarvotham, T. Kishino, N. Niikawa, E. Hidaka, T. Katsuyama, T. Higuchi, and J. Sagara. 1999. ASC, a novel 22-kDa protein, aggregates during apoptosis of human promyelocytic leukemia HL-60 cells. *J. Biol. Chem.* 274: 33835–33838.
36. Kanneganti, T. D., M. Body-Malapel, A. Amer, J. H. Park, J. Whitfield, Z. F. Taraporewala, D. Miller, J. T. Patton, N. Inohara, and G. Nunez. 2006. Critical role for cryopyrin/Nalp3 in activation of caspase-1 in response to viral infection and double-stranded RNA. *J. Biol. Chem.* 281: 36560–36568.
37. Paine, P. L., C. F. Austerberry, L. J. Desjarlais, and S. B. Horowitz. 1983. Protein loss during nuclear isolation. *J. Cell Biol.* 97: 1240–1242.
38. Gordon, J. S., J. Bruno, and J. J. Lucas. 1981. Heterogeneous binding of high mobility group chromosomal proteins to nuclei. *J. Cell Biol.* 88: 373–379.
39. Kanneganti, T. D., M. Lamkanfi, Y. G. Kim, G. Chen, J. H. Park, L. Franchi, P. Vandenabeele, and G. Nunez. 2007. Pannexin-1-mediated recognition of bacterial molecules activates the cryopyrin inflammasome independent of Toll-like receptor signaling. *Immunity* 26: 433–443.
40. Dowds, T. A., J. Masumoto, L. Zhu, N. Inohara, and G. Nunez. 2004. Cryopyrin-induced interleukin 1β secretion in monocytic cells: enhanced activity of disease-associated mutants and requirement for ASC. *J. Biol. Chem.* 279: 21924–21928.
41. Yu, J. W., J. Wu, Z. Zhang, P. Datta, I. Ibrahimi, S. Taniguchi, J. Sagara, T. Fernandes-Alnemri, and E. S. Alnemri. 2006. Cryopyrin and pyrin activate caspase-1, but not NF-κB, via ASC oligomerization. *Cell Death Differ.* 13: 236–249.
42. O'Connor, W., Jr., J. A. Harton, X. Zhu, M. W. Linhoff, and J. P. Ting. 2003. Cutting edge: CIAS1/cryopyrin/PYPAF1/NALP3/ CATERPILLER 1.1 is an inducible inflammatory mediator with NF-κB suppressive properties. *J. Immunol.* 171: 6329–6333.
43. Mileno, M. D., N. H. Margolis, B. D. Clark, C. A. Dinarello, J. F. Burke, and J. A. Gelfand. 1995. Coagulation of whole blood stimulates interleukin-1β gene expression. *J. Infect. Dis.* 172: 308–311.
44. Screaton, R. A., S. Kiessling, O. J. Sansom, C. B. Millar, K. Maddison, A. Bird, A. R. Clarke, and S. M. Frisch. 2003. Fas-associated death domain protein interacts with methyl-CpG binding domain protein 4: a potential link between genome surveillance and apoptosis. *Proc. Natl. Acad. Sci. USA* 100: 5211–5216.
45. Fernandes-Alnemri, T., J. Wu, J. W. Yu, P. Datta, B. Miller, W. Jankowski, S. Rosenberg, J. Zhang, and E. S. Alnemri. 2007. The pyroptosome: a supramolecular assembly of ASC dimers mediating inflammatory cell death via caspase-1 activation. *Cell Death Differ.* 14: 1590–1604.
46. Brough, D., and N. J. Rothwell. 2007. Caspase-1-dependent processing of pro-interleukin-1β is cytosolic and precedes cell death. *J. Cell Sci.* 120: 772–781.
47. Fink, S. L., and B. T. Cookson. 2006. Caspase-1-dependent pore formation during pyroptosis leads to osmotic lysis of infected host macrophages. *Cell. Microbiol.* 8: 1812–1825.
48. Suzuki, T., L. Franchi, C. Toma, H. Ashida, M. Ogawa, Y. Yoshikawa, H. Mimuro, N. Inohara, C. Sasakawa, and G. Nunez. 2007. Differential regulation of caspase-1 activation, pyroptosis, and autophagy via Ipaf and ASC in *Shigella*-infected macrophages. *PLoS Pathog.* 3: e111.
49. Willingham, S. B., D. T. Bergstralh, W. O'Connor, A. C. Morrison, D. J. Taxman, J. A. Duncan, S. Barnoy, M. M. Venkatesan, R. A. Flavell, M. Deshmukh, et al. 2007. Microbial pathogen-induced necrotic cell death mediated by the inflammasome components CIAS1/cryopyrin/NLRP3 and ASC. *Cell Host Microbe* 2: 147–159.
50. Ohtsuka, T., H. Ryu, Y. A. Minamishima, S. Macip, J. Sagara, K. I. Nakayama, S. A. Aaronson, and S. W. Lee. 2004. ASC is a Bax adaptor and regulates the p53-Bax mitochondrial apoptosis pathway. *Nat. Cell Biol.* 6: 121–128.
51. Singer, I. I., S. Scott, J. Chin, E. K. Bayne, G. Limjuco, J. Weidner, D. K. Miller, K. Chapman, and M. J. Kostura. 1995. The interleukin-1β-converting enzyme (ICE) is localized on the external cell surface membranes and in the cytoplasmic ground substance of human monocytes by immunoelectron microscopy. *J. Exp. Med.* 182: 1447–1459.
52. Rubartelli, A., F. Cozzolino, M. Talio, and R. Sitia. 1990. A novel secretory pathway for interleukin-1β, a protein lacking a signal sequence. *EMBO J.* 9: 1503–1510.
53. Mao, P.-L., Y. Jiang, B. Wee, and A. Porter. 1998. Activation of caspase-1 in the nucleus requires nuclear translocation of pro-caspase-1 mediated by its prodomain. *J. Biol. Chem.* 273: 23621–23624.
54. Shikama, Y. 2001. Comprehensive studies on subcellular localizations and cell death-inducing activities of eight GFP-tagged apoptosis-related caspases. *Exp. Cell Res.* 264: 315–325.
55. Nakagawara, A., Y. Nakamura, H. Ikeda, T. Hiwasa, K. Kuida, M. S. Su, H. Zhao, A. Cnaan, and S. Sakiyama. 1997. High levels of expression and nuclear localization of interleukin-1β converting enzyme (ICE) and CPP32 in favorable human neuroblastomas. *Cancer Res.* 57: 4578–4584.
56. Keller, M., A. Ruegg, S. Werner, and H. D. Beer. 2008. Active caspase-1 is a regulator of unconventional protein secretion. *Cell* 132: 818–831.
57. Gomez-Angelats, M., and J. A. Cidlowski. 2003. Molecular evidence for the nuclear localization of FADD. *Cell Death Differ.* 10: 791–797.
58. Alappat, E. C., C. Feig, B. Boyerinas, J. Volkland, M. Samuels, A. E. Murmann, A. Thorburn, V. J. Kidd, C. A. Slaughter, S. L. Osborn, et al. 2005. Phosphorylation of FADD at serine 194 by CKIα regulates its nonapoptotic activities. *Mol. Cell* 19: 321–332.
59. Morgan, M., J. Thorburn, P. P. Pandolfi, and A. Thorburn. 2002. Nuclear and cytoplasmic shuttling of TRADD induces apoptosis via different mechanisms. *J. Cell Biol.* 157: 975–984.
60. Wesemann, D. R., H. Qin, N. Kokorina, and E. N. Benveniste. 2004. TRADD interacts with STAT1-α and influences interferon-γ signaling. *Nat. Immunol.* 5: 199–207.